

## Multispectral Image Analysis Using Feature Extraction with Classification for Agricultural Crop Cultivation Based On 4G Wireless IOT Networks

**Prof. Dharmesh Dhabliya**

Department of Information Technology, Vishwakarma Institute of Information Technology  
dharmesh.dhabliya@viit.ac.in

Article History	Abstract
Received: 22 January 2020 Revised: 14 April 2020 Accepted: 19 May 2020	Land-use mapping and crop classification have both benefited greatly from the analysis of high-resolution remote sensing photos based on deep learning. This research proposes novel technique in multispectral image analysis based on feature extraction as well as classification utilizing DL architecture. The proposed model collects multispectral image based on agriculture crop cultivation by 4G IoT wireless networks. The input image has been processed for noise removal, smoothening and normalization. Then this processed image features have been extracted using stochastic Q-reinforcement neural network. the extracted features of multispectral image have been classified using discrete quantum convolutional architectures. Here the experimental analysis has been carried out for various agriculture crop cultivation-based dataset in terms of accuracy, precision, recall, F-1 score, RMSE, MAP and AUC. Keywords: multispectral image analysis, feature extraction, classification, deep learning, 4G IoT wireless networks
CC License	CC-BY-NC-SA

### 1. Introduction

The growing demand for food brought on by the planet's population boom, climate change, resource depletion, altered dietary preferences, and safety and health concerns are just a few of the obstacles that modern agriculture must overcome. The modernization of agriculture has the potential to guarantee environmental safety, maximum productivity, and sustainability [5] [6]. Acquisition and processing of farmland information are two essential requirements for PA [7]. High-performance sensors, such as RGB, multispectral, hyperspectral, thermal, and SAR cameras, have been used to examine physical and physiological changes in plants in both visible and invisible light for the purpose of gathering information about farms [8].

### 2. Related works

A key and basic component involved in an image classification process is feature extraction. Therefore, morphology, texture, and spectral reflectance are the key characteristics to concentrate on for precise weed identification. In work [9], a real-time computer vision system for weed recognition was demonstrated. As an extension of [10], a technique for identifying and categorising the primary citrus illnesses was described. The suggested method divided the disease-affected area using a colour difference algorithm. Earlier studies in lettuce fields, such those of [11] and [12], had good success identifying weeds and crops using RGB and multispectral imagery.

### 3. System model

This section discusses novel technique in multispectral image analysis based on feature extraction and classification using deep learning architecture. The proposed model collects multispectral image based on agriculture crop cultivation by 4G IoT wireless networks. The input image has been processed for noise removal, smoothening and normalization. Then this processed image features has been extracted using stochastic Q-reinforcement neural network. The extracted features of multispectral image have been classified using discrete quantum convolutional architectures. The proposed architecture is shown in figure-1.

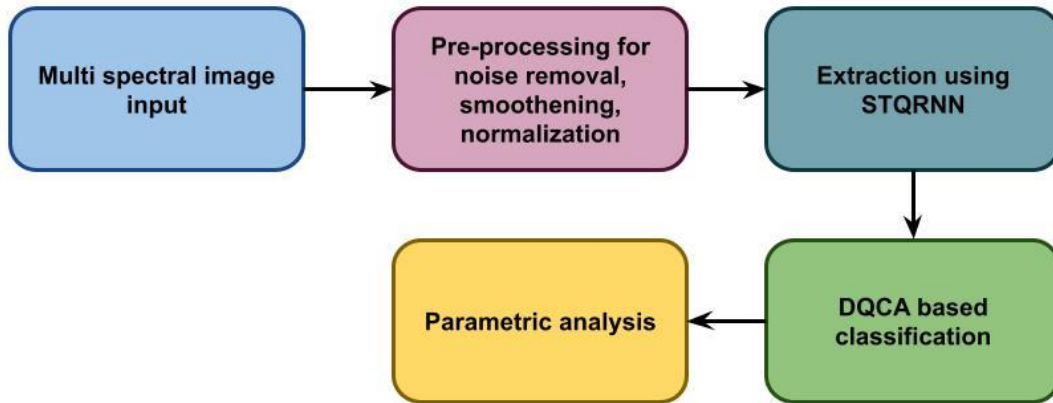


Figure 1: Overall proposed architecture

#### 3.1 Stochastic Q-reinforcement neural network-based feature extraction

Think of a binary classification issue where the examples are  $z = (x, y) \in \mathbb{R}^d \times \{-1, +1\}$ . It is possible to create a linear Q-learning classifier by reducing the primary cost function by eq. (1).

$$\mathcal{P}_n(\mathbf{w}) = \frac{\lambda}{2} \|\mathbf{w}\|^2 + \frac{1}{n} \sum_{i=1}^n \ell(y_i \mathbf{w}^\top \mathbf{x}_i) = \frac{1}{n} \sum_{i=1}^n \left( \frac{\lambda}{2} \|\mathbf{w}\|^2 + \ell(y_i \mathbf{w}^\top \mathbf{x}_i) \right) \quad (1)$$

$$\bar{\mathcal{U}} = \{ \mathbf{u} \in \mathbb{R}^n \text{ such that } \mathbf{u} = \sum_{j=1}^m \alpha_j \mathbf{u}_j; \alpha_j \in \mathbb{R}^+ (\forall j); \sum_{j=1}^m \alpha_j = 1 \}$$

The related scalar product of a n by n real-symmetric positive-definite matrix eq. (2)

$$(\mathbf{u}, \mathbf{v}) = \mathbf{u}^\top \mathbf{A}_n \mathbf{v} \quad (\mathbf{u}, \mathbf{v} \in \mathbb{R}^n),$$

$$\|\mathbf{u}\| = \sqrt{\mathbf{u}^\top \mathbf{A}_n \mathbf{u}},$$

$$\xi_s = \frac{1}{2}(\xi_2 + \xi_1), \quad \xi_d = \frac{1}{2}(\xi_2 - \xi_1)(\xi_1, \xi_d) = \frac{1}{4}(\xi_2 + \xi_1, \xi_2 - \xi_1) = \frac{1}{4}(\|\xi_2\|^2 - \|\xi_1\|^2) = 0 \quad (2)$$

Hence  $\xi_n \perp \xi_d$ , and since  $\xi_s \in \bar{\mathcal{U}}, \|\xi_s\| \geq \mu$ , and by eq. (3)

$$\mu^2 = \|\xi_2\|^2 = \|\xi_s + \xi_d\|^2 = \|\xi_s\|^2 + \|\xi_d\|^2 \geq \mu^2 + \|\xi_d\|^2 \Rightarrow \xi_d = 0 \quad (3)$$

Variable  $h_t$  is a random number, and the equation calculates the separation between the present solution,  $w^t$ , and the ideal solution,  $w^*$ . The convergence rate of SGD may therefore be calculated using eq. (4):

$$h_{t+1} - h_t = \|\mathbf{w}^{t+1} - \mathbf{w}^*\|_2^2 - \|\mathbf{w}^t - \mathbf{w}^*\|_2^2 = (w^{t+1} + w^t - 2w^*)(w^{t+1} - w^t) = (2w^t - 2w^* - \eta_t \nabla \psi_w(\mathbf{d}_t))(-\eta_t \nabla \psi_w(\mathbf{d}_t)) \quad \infty = -2\eta_t(\mathbf{w}^t - \mathbf{w}^*) \nabla \psi_w(\mathbf{d}_t) + \eta_t^2 (\nabla \psi_w(\mathbf{d}_t))^2 \quad (4)$$

#### 3.2 Discrete Quantum Convolutional Architectures

The subsequent function can be used to define the discrete Wavelet transform by eq. (5), (6):

$$\begin{aligned} \psi_{j,k}(t) &= 2^{\frac{j}{2}}\psi(2^j t - k), j, k \in Z; z = \{0,1,2, \dots\}. \\ \phi(t) &= \sqrt{2}\sum_k l_k \phi(2t - k) \\ \psi(t) &= \sqrt{2}\sum_k h_k \phi(2t - k) \end{aligned} \quad (5)$$

where:  $w(t) = [w_0(t), w_1(t), \dots, w_{M-1}]^T$   
 $\Downarrow 2^{k-1} = s, f(t) = \sum_{n=1}^s \sum_{m=0}^{M-1} A_{n,m} w_{n,m}(t) = A^T w_{n,m}(t)$  (6)

The output of the QNN can be described using qubit-controlled NOT-gate U(cj) as the transfer function of hidden layer in eq. (7).

$$\begin{aligned} y_k &= g\left(\sum_{j=1}^m w_{jk} h_j\right) = g\left(\sum_{j=1}^m w_{jk} \sin\left(\frac{\pi}{2} f(\gamma_j)\right.\right. \\ &\quad \left.\left.- \arg\left(\sum_{i=1}^m R(\theta_{ij})|x_i\rangle\right)\right)\right) \end{aligned} \quad (7)$$

here  $i = 1,2, \dots, n; j = 1,2, \dots, m; \text{ and } k = 1,2, \dots, p$ .

#### 4. Performance analysis

This section discusses about the parametric analysis of proposed Multispectral image analysis for agriculture crop cultivation based on deep learning techniques. The simulations simulate a synthetic data collection issue in a 30 m x 30 m area and were ran in MATLAB with a 1.8 GHz Intel i7 processor and 16 GB of RAM.

Table 1: Comparison of proposed and existing methods

Parameter	ICPE	CDA	MISFE_ACC_4G_IoT
Accuracy	82	88	96
Precision	72	76	81
Recall	65	68	71
F1_Score	55	59	65
RMSE	42	44	46
MAP	51	53	55
AUC	32	36	41

The above table-1 shows comparative analysis between proposed and existing techniques in terms of accuracy, precision, recall, F-1 score, RMSE, MAP and AUC. Here the analysis has been carried out based on number of epochs. Accuracy calculation is done by the general prediction capability of projected DL method. For calculating F-score, number of images processed are EEG signal for both existing and proposed technique. The F-score reveals each feature ability to discriminate independently from other features. For the first feature, a score is generated, and for the second feature, a different score is obtained. However, it says nothing about how the two elements work together. Here, calculating the F-score using exploitation has determined the prediction performance. It is created by looking at the harmonic component of recall and precision. If the calculated score is 1, it is considered excellent, whereas a score of 0 indicates poor performance. The actual negative rate is not taken into consideration by F-measures. The accuracy of a class is calculated by dividing the total items classified as belonging to positive class by number of true positives. Probability that a classification function will produce a true positive rate when present. It is also known by the acronym TP amount. In this context, recall is described as ratio of total number of components that genuinely fall into a positive class to several true positives. How well a method can recognise Positive samples is calculated by recall. Recall increases as more positive samples are determined. When training regression or time series models, RMSE is one of the most widely used metrics to gauge how accurately our forecasting model predicts values compared to real or observed values. MSE squared root is used to calculate RMSE. The RMSE calculates the change in each pixel as a result of processing.

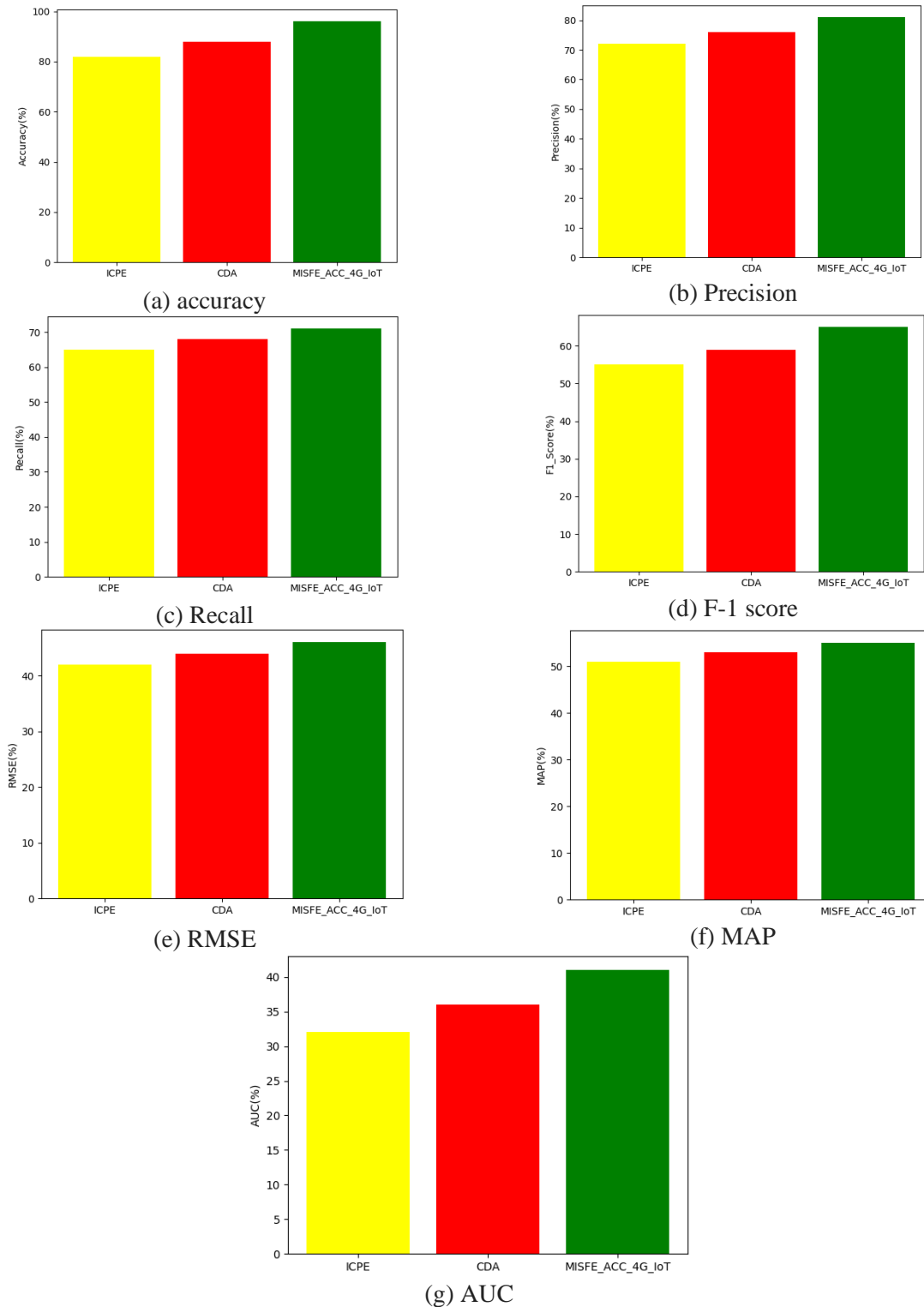


Figure-2 Comparative analysis between proposed and existing technique in terms of (a) accuracy, (b) Precision, (c) Recall, (d) F-1 score, (e) RMSE, (f) MAP, (g) AUC

From above figure 2 (a)- (g) shows comparative analysis between proposed and existing technique. the proposed technique attained accuracy of 96%, precision of 81%, recall of 71%, F-1 score of 65%, RMSE of 46%, MAP of 55% and AUC of 41%. While the existing ICPE attained accuracy of 82%, precision of 72%, recall of 65%, F-1 score of 55%, RMSE of 42%, MAP of 51% and AUC of 32%; CDA attained accuracy of 88%, precision of 76%, recall of 68%, F-1 score of 59%, RMSE of 44%, MAP of 53% and AUC of 36%.

## 5. Conclusion

This research proposes novel technique in multispectral image analysis based on feature extraction with classification. The collected input processed data features have been extracted using stochastic Q-reinforcement neural network and classified using discrete quantum convolutional architectures. Here the experimental analysis has been carried out for various agriculture crop cultivation-based dataset in terms of accuracy, precision, recall, F-1 score, RMSE, MAP and AUC. the proposed technique attained accuracy of 96%, precision of 81%, recall of 71%, F-1 score of 65%, RMSE of 46%, MAP of 55% and AUC of 41%. The future scope of this research can be extended to various image analysis with enhanced accuracy.

## Reference

- [1] Han, X. (2018). A Mathematical Introduction to Reinforcement Learning.
- [2] Bottou, L. (2010). Large-scale machine learning with stochastic gradient descent. In *Proceedings of COMPSTAT'2010* (pp. 177-186). Physica-Verlag HD.
- [3] Wang, L., Yang, Y., Min, R., & Chakradhar, S. (2017). Accelerating deep neural network training with inconsistent stochastic gradient descent. *Neural Networks*, 93, 219-229.
- [4] Mercier, Q., Poirion, F., & Désidéri, J. A. (2018). A stochastic multiple gradient descent algorithm. *European Journal of Operational Research*, 271(3), 808-817.
- [5] Guan, W., Zhou, H., Su, Z., Zhang, X., & Zhao, C. (2019). Ship steering control based on quantum neural network. *Complexity*, 2019.
- [6] Yaloveha, V., Hlavcheva, D., & Podorozhniak, A. (2019). Usage of convolutional neural network for multispectral image processing applied to the problem of detecting fire hazardous forest areas.
- [7] Sa, I., Popović, M., Khanna, R., Chen, Z., Lottes, P., Liebisch, F., ... & Siegart, R. (2018). WeedMap: A large-scale semantic weed mapping framework using aerial multispectral imaging and deep neural network for precision farming. *Remote Sensing*, 10(9), 1423.
- [8] Romero, M., Luo, Y., Su, B., & Fuentes, S. (2018). Vineyard water status estimation using multispectral imagery from an UAV platform and machine learning algorithms for irrigation scheduling management. *Computers and electronics in agriculture*, 147, 109-117.
- [9] Tsakanikas, P., Pavlidis, D., & Nychas, G. J. (2015). High throughput multispectral image processing with applications in food science. *PloS one*, 10(10), e0140122.
- [10] Zhang, B., Zhang, C., Li, G., Lin, L., Zhang, C., Wang, F., & Yan, W. (2019). Multispectral heterogeneity detection based on frame accumulation and deep learning. *IEEE Access*, 7, 29277-29284.
- [11] Estelles-Lopez, L., Ropodi, A., Pavlidis, D., Fotopoulou, J., Gkousari, C., Peyrodie, A., ... & Mohareb, F. (2017). An automated ranking platform for machine learning regression models for meat spoilage prediction using multi-spectral imaging and metabolic profiling. *Food research international*, 99, 206-215.
- [12] Mou, L., & Zhu, X. X. (2016, July). Spatiotemporal scene interpretation of space videos via deep neural network and tracklet analysis. In *2016 IEEE International Geoscience and Remote Sensing Symposium (IGARSS)* (pp. 1823-1826). IEEE.